BABAR-PUB-06/022
SLAC-PUB-11854
hep-ex/0605037

Search for $B^+ \to \phi\pi^+$ and $B^0 \to \phi\pi^0$ Decays

B. Aubert,[1] R. Barate,[1] M. Bona,[1] D. Boutigny,[1] F. Couderc,[1] Y. Karyotakis,[1] J. P. Lees,[1] V. Poireau,[1] V. Tisserand,[1] A. Zghiche,[1] E. Grauges,[2] A. Palano,[3] M. Pappagallo,[3] J. C. Chen,[4] N. D. Qi,[4] G. Rong,[4] P. Wang,[4] Y. S. Zhu,[4] G. Eigen,[5] I. Ofte,[5] B. Stugu,[5] G. S. Abrams,[6] M. Battaglia,[6] D. N. Brown,[6] J. Button-Shafer,[6] R. N. Cahn,[6] E. Charles,[6] C. T. Day,[6] M. S. Gill,[6] Y. Groysman,[6] R. G. Jacobsen,[6] J. A. Kadyk,[6] L. T. Kerth,[6] Yu. G. Kolomensky,[6] G. Kukartsev,[6] G. Lynch,[6] L. M. Mir,[6] P. J. Oddone,[6] T. J. Orimoto,[6] M. Pripstein,[6] N. A. Roe,[6] M. T. Ronan,[6] W. A. Wenzel,[6] M. Barrett,[7] K. E. Ford,[7] T. J. Harrison,[7] A. J. Hart,[7] C. M. Hawkes,[7] S. E. Morgan,[7] A. T. Watson,[7] K. Goetzen,[8] T. Held,[8] H. Koch,[8] B. Lewandowski,[8] M. Pelizaeus,[8] K. Peters,[8] T. Schroeder,[8] M. Steinke,[8] J. T. Boyd,[9] J. P. Burke,[9] W. N. Cottingham,[9] D. Walker,[9] T. Cuhadar-Donszelmann,[10] B. G. Fulsom,[10] C. Hearty,[10] N. S. Knecht,[10] T. S. Mattison,[10] J. A. McKenna,[10] A. Khan,[11] P. Kyberd,[11] M. Saleem,[11] L. Teodorescu,[11] V. E. Blinov,[12] A. D. Bukin,[12] V. P. Druzhinin,[12] V. B. Golubev,[12] A. P. Onuchin,[12] S. I. Serednyakov,[12] Yu. I. Skovpen,[12] E. P. Solodov,[12] K. Yu Todyshev,[12] D. S. Best,[13] M. Bondioli,[13] M. Bruinsma,[13] M. Chao,[13] S. Curry,[13] I. Eschrich,[13] D. Kirkby,[13] A. J. Lankford,[13] P. Lund,[13] M. Mandelkern,[13] R. K. Mommsen,[13] W. Roethel,[13] D. P. Stoker,[13] S. Abachi,[14] C. Buchanan,[14] S. D. Foulkes,[15] J. W. Gary,[15] O. Long,[15] B. C. Shen,[15] K. Wang,[15] L. Zhang,[15] H. K. Hadavand,[16] E. J. Hill,[16] H. P. Paar,[16] S. Rahatlou,[16] V. Sharma,[16] J. W. Berryhill,[17] C. Campagnari,[17] A. Cunha,[17] B. Dahmes,[17] T. M. Hong,[17] D. Kovalskyi,[17] J. D. Richman,[17] T. W. Beck,[18] A. M. Eisner,[18] C. J. Flacco,[18] C. A. Heusch,[18] J. Kroseberg,[18] W. S. Lockman,[18] G. Nesom,[18] T. Schalk,[18] B. A. Schumm,[18] A. Seiden,[18] P. Spradlin,[18] D. C. Williams,[18] M. G. Wilson,[18] J. Albert,[19] E. Chen,[19] A. Dvoretskii,[19] D. G. Hitlin,[19] I. Narsky,[19] T. Piatenko,[19] F. C. Porter,[19] A. Ryd,[19] A. Samuel,[19] R. Andreassen,[20] G. Mancinelli,[20] B. T. Meadows,[20] M. D. Sokoloff,[20] F. Blanc,[21] P. C. Bloom,[21] S. Chen,[21] W. T. Ford,[21] J. F. Hirschauer,[21] A. Kreisel,[21] U. Nauenberg,[21] A. Olivas,[21] W. O. Ruddick,[21] J. G. Smith,[21] K. A. Ulmer,[21] S. R. Wagner,[21] J. Zhang,[21] A. Chen,[22] E. A. Eckhart,[22] A. Soffer,[22] W. H. Toki,[22] R. J. Wilson,[22] F. Winklmeier,[22] Q. Zeng,[22] D. D. Altenburg,[23] E. Feltresi,[23] A. Hauke,[23] H. Jasper,[23] B. Spaan,[23] T. Brandt,[24] V. Klose,[24] H. M. Lacker,[24] W. F. Mader,[24] R. Nogowski,[24] A. Petzold,[24] J. Schubert,[24] K. R. Schubert,[24] R. Schwierz,[24] J. E. Sundermann,[24] A. Volk,[24] D. Bernard,[25] G. R. Bonneaud,[25] P. Grenier,[25,*] E. Latour,[25] Ch. Thiebaux,[25] M. Verderi,[25] D. J. Bard,[26] P. J. Clark,[26] W. Gradl,[26] F. Muheim,[26] S. Playfer,[26] A. I. Robertson,[26] Y. Xie,[26] M. Andreotti,[27] D. Bettoni,[27] C. Bozzi,[27] R. Calabrese,[27] G. Cibinetto,[27] E. Luppi,[27] M. Negrini,[27] A. Petrella,[27] L. Piemontese,[27] E. Prencipe,[27] F. Anulli,[28] R. Baldini-Ferroli,[28] A. Calcaterra,[28] R. de Sangro,[28] G. Finocchiaro,[28] S. Pacetti,[28] P. Patteri,[28] I. M. Peruzzi,[28,†] M. Piccolo,[28] M. Rama,[28] A. Zallo,[28] A. Buzzo,[29] R. Capra,[29] R. Contri,[29] M. Lo Vetere,[29] M. M. Macri,[29] M. R. Monge,[29] S. Passaggio,[29] C. Patrignani,[29] E. Robutti,[29] A. Santroni,[29] S. Tosi,[29] G. Brandenburg,[30] K. S. Chaisanguanthum,[30] M. Morii,[30] J. Wu,[30] R. S. Dubitzky,[31] J. Marks,[31] S. Schenk,[31] U. Uwer,[31] W. Bhimji,[32] D. A. Bowerman,[32] P. D. Dauncey,[32] U. Egede,[32] R. L. Flack,[32] J. R. Gaillard,[32] J .A. Nash,[32] M. B. Nikolich,[32] W. Panduro Vazquez,[32] X. Chai,[33] M. J. Charles,[33] U. Mallik,[33] N. T. Meyer,[33] V. Ziegler,[33] J. Cochran,[34] H. B. Crawley,[34] L. Dong,[34] V. Eyges,[34] W. T. Meyer,[34] S. Prell,[34] E. I. Rosenberg,[34] A. E. Rubin,[34] A. V. Gritsan,[35] M. Fritsch,[36] G. Schott,[36] N. Arnaud,[37] M. Davier,[37] G. Grosdidier,[37] A. Höcker,[37] F. Le Diberder,[37] V. Lepeltier,[37] A. M. Lutz,[37] A. Oyanguren,[37] S. Pruvot,[37] S. Rodier,[37] P. Roudeau,[37] M. H. Schune,[37] A. Stocchi,[37] W. F. Wang,[37] G. Wormser,[37] C. H. Cheng,[38] D. J. Lange,[38] D. M. Wright,[38] C. A. Chavez,[39] I. J. Forster,[39] J. R. Fry,[39] E. Gabathuler,[39] R. Gamet,[39] K. A. George,[39] D. E. Hutchcroft,[39] D. J. Payne,[39] K. C. Schofield,[39] C. Touramanis,[39] A. J. Bevan,[40] F. Di Lodovico,[40] W. Menges,[40] R. Sacco,[40] C. L. Brown,[41] G. Cowan,[41] H. U. Flaecher,[41] D. A. Hopkins,[41] P. S. Jackson,[41] T. R. McMahon,[41] S. Ricciardi,[41] F. Salvatore,[41] D. N. Brown,[42] C. L. Davis,[42] J. Allison,[43] N. R. Barlow,[43] R. J. Barlow,[43] Y. M. Chia,[43] C. L. Edgar,[43] M. P. Kelly,[43] G. D. Lafferty,[43] M. T. Naisbit,[43] J. C. Williams,[43] J. I. Yi,[43] C. Chen,[44] W. D. Hulsbergen,[44] A. Jawahery,[44] C. K. Lae,[44] D. A. Roberts,[44] G. Simi,[44] G. Blaylock,[45] C. Dallapiccola,[45] S. S. Hertzbach,[45] X. Li,[45] T. B. Moore,[45] S. Saremi,[45] H. Staengle,[45] S. Y. Willocq,[45] R. Cowan,[46] K. Koeneke,[46] G. Sciolla,[46] S. J. Sekula,[46] M. Spitznagel,[46]

Submitted to Physical Review D

Work supported in part by Department of Energy contract DE-AC02-76SF00515

F. Taylor,[46] R. K. Yamamoto,[46] H. Kim,[47] P. M. Patel,[47] C. T. Potter,[47] S. H. Robertson,[47] A. Lazzaro,[48] V. Lombardo,[48] F. Palombo,[48] J. M. Bauer,[49] L. Cremaldi,[49] V. Eschenburg,[49] R. Godang,[49] R. Kroeger,[49] J. Reidy,[49] D. A. Sanders,[49] D. J. Summers,[49] H. W. Zhao,[49] S. Brunet,[50] D. Côté,[50] M. Simard,[50] P. Taras,[50] F. B. Viaud,[50] H. Nicholson,[51] N. Cavallo,[52, ‡] G. De Nardo,[52] D. del Re,[52] F. Fabozzi,[52, ‡] C. Gatto,[52] L. Lista,[52] D. Monorchio,[52] P. Paolucci,[52] D. Piccolo,[52] C. Sciacca,[52] M. Baak,[53] H. Bulten,[53] G. Raven,[53] H. L. Snoek,[53] C. P. Jessop,[54] J. M. LoSecco,[54] T. Allmendinger,[55] G. Benelli,[55] K. K. Gan,[55] K. Honscheid,[55] D. Hufnagel,[55] P. D. Jackson,[55] H. Kagan,[55] R. Kass,[55] T. Pulliam,[55] A. M. Rahimi,[55] R. Ter-Antonyan,[55] Q. K. Wong,[55] N. L. Blount,[56] J. Brau,[56] R. Frey,[56] O. Igonkina,[56] M. Lu,[56] R. Rahmat,[56] N. B. Sinev,[56] D. Strom,[56] J. Strube,[56] E. Torrence,[56] F. Galeazzi,[57] A. Gaz,[57] M. Margoni,[57] M. Morandin,[57] A. Pompili,[57] M. Posocco,[57] M. Rotondo,[57] F. Simonetto,[57] R. Stroili,[57] C. Voci,[57] M. Benayoun,[58] J. Chauveau,[58] P. David,[58] L. Del Buono,[58] Ch. de la Vaissière,[58] O. Hamon,[58] B. L. Hartfiel,[58] M. J. J. John,[58] Ph. Leruste,[58] J. Malclès,[58] J. Ocariz,[58] L. Roos,[58] G. Therin,[58] P. K. Behera,[59] L. Gladney,[59] J. Panetta,[59] M. Biasini,[60] R. Covarelli,[60] M. Pioppi,[60] C. Angelini,[61] G. Batignani,[61] S. Bettarini,[61] F. Bucci,[61] G. Calderini,[61] M. Carpinelli,[61] R. Cenci,[61] F. Forti,[61] M. A. Giorgi,[61] A. Lusiani,[61] G. Marchiori,[61] M. A. Mazur,[61] M. Morganti,[61] N. Neri,[61] E. Paoloni,[61] G. Rizzo,[61] J. Walsh,[61] M. Haire,[62] D. Judd,[62] D. E. Wagoner,[62] J. Biesiada,[63] N. Danielson,[63] P. Elmer,[63] Y. P. Lau,[63] C. Lu,[63] J. Olsen,[63] A. J. S. Smith,[63] A. V. Telnov,[63] F. Bellini,[64] G. Cavoto,[64] A. D'Orazio,[64] E. Di Marco,[64] R. Faccini,[64] F. Ferrarotto,[64] F. Ferroni,[64] M. Gaspero,[64] L. Li Gioi,[64] M. A. Mazzoni,[64] S. Morganti,[64] G. Piredda,[64] F. Polci,[64] F. Safai Tehrani,[64] C. Voena,[64] M. Ebert,[65] H. Schröder,[65] R. Waldi,[65] T. Adye,[66] N. De Groot,[66] B. Franek,[66] E. O. Olaiya,[66] F. F. Wilson,[66] S. Emery,[67] A. Gaidot,[67] S. F. Ganzhur,[67] G. Hamel de Monchenault,[67] W. Kozanecki,[67] M. Legendre,[67] B. Mayer,[67] G. Vasseur,[67] Ch. Yèche,[67] M. Zito,[67] W. Park,[68] M. V. Purohit,[68] A. W. Weidemann,[68] J. R. Wilson,[68] M. T. Allen,[69] D. Aston,[69] R. Bartoldus,[69] P. Bechtle,[69] N. Berger,[69] A. M. Boyarski,[69] R. Claus,[69] J. P. Coleman,[69] M. R. Convery,[69] M. Cristinziani,[69] J. C. Dingfelder,[69] D. Dong,[69] J. Dorfan,[69] G. P. Dubois-Felsmann,[69] D. Dujmic,[69] W. Dunwoodie,[69] R. C. Field,[69] T. Glanzman,[69] S. J. Gowdy,[69] M. T. Graham,[69] V. Halyo,[69] C. Hast,[69] T. Hryn'ova,[69] W. R. Innes,[69] M. H. Kelsey,[69] P. Kim,[69] M. L. Kocian,[69] D. W. G. S. Leith,[69] S. Li,[69] J. Libby,[69] S. Luitz,[69] V. Luth,[69] H. L. Lynch,[69] D. B. MacFarlane,[69] H. Marsiske,[69] R. Messner,[69] D. R. Muller,[69] C. P. O'Grady,[69] V. E. Ozcan,[69] A. Perazzo,[69] M. Perl,[69] B. N. Ratcliff,[69] A. Roodman,[69] A. A. Salnikov,[69] R. H. Schindler,[69] J. Schwiening,[69] A. Snyder,[69] J. Stelzer,[69] D. Su,[69] M. K. Sullivan,[69] K. Suzuki,[69] S. K. Swain,[69] J. M. Thompson,[69] J. Va'vra,[69] N. van Bakel,[69] M. Weaver,[69] A. J. R. Weinstein,[69] W. J. Wisniewski,[69] M. Wittgen,[69] D. H. Wright,[69] A. K. Yarritu,[69] K. Yi,[69] C. C. Young,[69] P. R. Burchat,[70] A. J. Edwards,[70] S. A. Majewski,[70] B. A. Petersen,[70] C. Roat,[70] L. Wilden,[70] S. Ahmed,[71] M. S. Alam,[71] R. Bula,[71] J. A. Ernst,[71] V. Jain,[71] B. Pan,[71] M. A. Saeed,[71] F. R. Wappler,[71] S. B. Zain,[71] W. Bugg,[72] M. Krishnamurthy,[72] S. M. Spanier,[72] R. Eckmann,[73] J. L. Ritchie,[73] A. Satpathy,[73] C. J. Schilling,[73] R. F. Schwitters,[73] J. M. Izen,[74] I. Kitayama,[74] X. C. Lou,[74] S. Ye,[74] F. Bianchi,[75] F. Gallo,[75] D. Gamba,[75] M. Bomben,[76] L. Bosisio,[76] C. Cartaro,[76] F. Cossutti,[76] G. Della Ricca,[76] S. Dittongo,[76] S. Grancagnolo,[76] L. Lanceri,[76] L. Vitale,[76] V. Azzolini,[77] F. Martinez-Vidal,[77] Sw. Banerjee,[78] B. Bhuyan,[78] C. M. Brown,[78] D. Fortin,[78] K. Hamano,[78] R. Kowalewski,[78] I. M. Nugent,[78] J. M. Roney,[78] R. J. Sobie,[78] J. J. Back,[79] P. F. Harrison,[79] T. E. Latham,[79] G. B. Mohanty,[79] H. R. Band,[80] X. Chen,[80] B. Cheng,[80] S. Dasu,[80] M. Datta,[80] A. M. Eichenbaum,[80] K. T. Flood,[80] J. J. Hollar,[80] J. R. Johnson,[80] P. E. Kutter,[80] H. Li,[80] R. Liu,[80] B. Mellado,[80] A. Mihalyi,[80] A. K. Mohapatra,[80] Y. Pan,[80] M. Pierini,[80] R. Prepost,[80] P. Tan,[80] S. L. Wu,[80] Z. Yu,[80] and H. Neal[81]

(The *BABAR* Collaboration)

[1] *Laboratoire de Physique des Particules, F-74941 Annecy-le-Vieux, France*
[2] *Universitat de Barcelona, Facultat de Fisica Dept. ECM, E-08028 Barcelona, Spain*
[3] *Università di Bari, Dipartimento di Fisica and INFN, I-70126 Bari, Italy*
[4] *Institute of High Energy Physics, Beijing 100039, China*
[5] *University of Bergen, Institute of Physics, N-5007 Bergen, Norway*
[6] *Lawrence Berkeley National Laboratory and University of California, Berkeley, California 94720, USA*
[7] *University of Birmingham, Birmingham, B15 2TT, United Kingdom*
[8] *Ruhr Universität Bochum, Institut für Experimentalphysik 1, D-44780 Bochum, Germany*
[9] *University of Bristol, Bristol BS8 1TL, United Kingdom*
[10] *University of British Columbia, Vancouver, British Columbia, Canada V6T 1Z1*
[11] *Brunel University, Uxbridge, Middlesex UB8 3PH, United Kingdom*
[12] *Budker Institute of Nuclear Physics, Novosibirsk 630090, Russia*
[13] *University of California at Irvine, Irvine, California 92697, USA*
[14] *University of California at Los Angeles, Los Angeles, California 90024, USA*

[15] University of California at Riverside, Riverside, California 92521, USA
[16] University of California at San Diego, La Jolla, California 92093, USA
[17] University of California at Santa Barbara, Santa Barbara, California 93106, USA
[18] University of California at Santa Cruz, Institute for Particle Physics, Santa Cruz, California 95064, USA
[19] California Institute of Technology, Pasadena, California 91125, USA
[20] University of Cincinnati, Cincinnati, Ohio 45221, USA
[21] University of Colorado, Boulder, Colorado 80309, USA
[22] Colorado State University, Fort Collins, Colorado 80523, USA
[23] Universität Dortmund, Institut für Physik, D-44221 Dortmund, Germany
[24] Technische Universität Dresden, Institut für Kern- und Teilchenphysik, D-01062 Dresden, Germany
[25] Ecole Polytechnique, LLR, F-91128 Palaiseau, France
[26] University of Edinburgh, Edinburgh EH9 3JZ, United Kingdom
[27] Università di Ferrara, Dipartimento di Fisica and INFN, I-44100 Ferrara, Italy
[28] Laboratori Nazionali di Frascati dell'INFN, I-00044 Frascati, Italy
[29] Università di Genova, Dipartimento di Fisica and INFN, I-16146 Genova, Italy
[30] Harvard University, Cambridge, Massachusetts 02138, USA
[31] Universität Heidelberg, Physikalisches Institut, Philosophenweg 12, D-69120 Heidelberg, Germany
[32] Imperial College London, London, SW7 2AZ, United Kingdom
[33] University of Iowa, Iowa City, Iowa 52242, USA
[34] Iowa State University, Ames, Iowa 50011-3160, USA
[35] Johns Hopkins University, Baltimore, Maryland 21218, USA
[36] Universität Karlsruhe, Institut für Experimentelle Kernphysik, D-76021 Karlsruhe, Germany
[37] Laboratoire de l'Accélérateur Linéaire, IN2P3-CNRS et Université Paris-Sud 11,
Centre Scientifique d'Orsay, B.P. 34, F-91898 ORSAY Cedex, France
[38] Lawrence Livermore National Laboratory, Livermore, California 94550, USA
[39] University of Liverpool, Liverpool L69 7ZE, United Kingdom
[40] Queen Mary, University of London, E1 4NS, United Kingdom
[41] University of London, Royal Holloway and Bedford New College, Egham, Surrey TW20 0EX, United Kingdom
[42] University of Louisville, Louisville, Kentucky 40292, USA
[43] University of Manchester, Manchester M13 9PL, United Kingdom
[44] University of Maryland, College Park, Maryland 20742, USA
[45] University of Massachusetts, Amherst, Massachusetts 01003, USA
[46] Massachusetts Institute of Technology, Laboratory for Nuclear Science, Cambridge, Massachusetts 02139, USA
[47] McGill University, Montréal, Québec, Canada H3A 2T8
[48] Università di Milano, Dipartimento di Fisica and INFN, I-20133 Milano, Italy
[49] University of Mississippi, University, Mississippi 38677, USA
[50] Université de Montréal, Physique des Particules, Montréal, Québec, Canada H3C 3J7
[51] Mount Holyoke College, South Hadley, Massachusetts 01075, USA
[52] Università di Napoli Federico II, Dipartimento di Scienze Fisiche and INFN, I-80126, Napoli, Italy
[53] NIKHEF, National Institute for Nuclear Physics and High Energy Physics, NL-1009 DB Amsterdam, The Netherlands
[54] University of Notre Dame, Notre Dame, Indiana 46556, USA
[55] Ohio State University, Columbus, Ohio 43210, USA
[56] University of Oregon, Eugene, Oregon 97403, USA
[57] Università di Padova, Dipartimento di Fisica and INFN, I-35131 Padova, Italy
[58] Universités Paris VI et VII, Laboratoire de Physique Nucléaire et de Hautes Energies, F-75252 Paris, France
[59] University of Pennsylvania, Philadelphia, Pennsylvania 19104, USA
[60] Università di Perugia, Dipartimento di Fisica and INFN, I-06100 Perugia, Italy
[61] Università di Pisa, Dipartimento di Fisica, Scuola Normale Superiore and INFN, I-56127 Pisa, Italy
[62] Prairie View A&M University, Prairie View, Texas 77446, USA
[63] Princeton University, Princeton, New Jersey 08544, USA
[64] Università di Roma La Sapienza, Dipartimento di Fisica and INFN, I-00185 Roma, Italy
[65] Universität Rostock, D-18051 Rostock, Germany
[66] Rutherford Appleton Laboratory, Chilton, Didcot, Oxon, OX11 0QX, United Kingdom
[67] DSM/Dapnia, CEA/Saclay, F-91191 Gif-sur-Yvette, France
[68] University of South Carolina, Columbia, South Carolina 29208, USA
[69] Stanford Linear Accelerator Center, Stanford, California 94309, USA
[70] Stanford University, Stanford, California 94305-4060, USA
[71] State University of New York, Albany, New York 12222, USA
[72] University of Tennessee, Knoxville, Tennessee 37996, USA
[73] University of Texas at Austin, Austin, Texas 78712, USA
[74] University of Texas at Dallas, Richardson, Texas 75083, USA
[75] Università di Torino, Dipartimento di Fisica Sperimentale and INFN, I-10125 Torino, Italy
[76] Università di Trieste, Dipartimento di Fisica and INFN, I-34127 Trieste, Italy
[77] IFIC, Universitat de Valencia-CSIC, E-46071 Valencia, Spain

[78] University of Victoria, Victoria, British Columbia, Canada V8W 3P6
[79] Department of Physics, University of Warwick, Coventry CV4 7AL, United Kingdom
[80] University of Wisconsin, Madison, Wisconsin 53706, USA
[81] Yale University, New Haven, Connecticut 06511, USA

(Dated: May 19, 2006)

A search has been made for the decays $B^+ \to \phi\pi^+$ and $B^0 \to \phi\pi^0$ in a data sample of approximately 232 $\times 10^6$ $B\bar{B}$ pairs recorded at the $\Upsilon(4S)$ resonance with the *BABAR* detector at the PEP-II B-meson Factory at SLAC. No significant signals have been observed, and therefore upper limits have been set on the branching fractions: $\mathcal{B}(B^+ \to \phi\pi^+) < 2.4\times10^{-7}$ and $\mathcal{B}(B^0 \to \phi\pi^0) < 2.8\times10^{-7}$ at 90% probability.

PACS numbers: 13.25.Hw, 12.15.Hh, 11.30.Er

The measurements of $B \to \phi K$ and $B \to \phi\pi$ decay rates are important because they are sensitive to contributions beyond the Standard Model (SM). In particular, the latter is strongly suppressed in the SM, and a measurement of $\mathcal{B}(B \to \phi\pi) \gtrsim 10^{-7}$ would be evidence for new physics, for example supersymmetric contributions [1]. The study of the processes $B^+ \to \phi\pi^+$ [2] and $B^0 \to \phi\pi^0$ is also important to understand the theoretical uncertainties associated with measurements of *CP* asymmetries in $B^0 \to \phi K^0$ decays. The $B \to \phi\pi$ decay amplitudes are related to the sub-leading terms of the $B^0 \to \phi K^0$ decay amplitude [3] and can therefore provide stringent bounds on possible contributions to the time-dependent *CP* asymmetry in $B^0 \to \phi K^0$ [4], another probe of new physics effects in B decays.

In Fig. 1 we show the leading order Feynman diagram for the $B \to \phi\pi$ decay and a sub-leading diagram for $B \to \phi K$ decay.

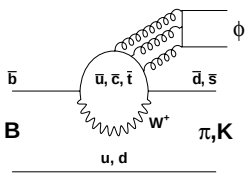

FIG. 1: Feynman diagram for $B \to \phi\pi$ and $B \to \phi K$.

Previous searches for these decay modes have been reported by *BABAR* and CLEO [5–7]. The results presented here are based on data collected with the *BABAR* detector [8] at the PEP-II asymmetric-energy e^+e^- collider [9] located at the Stanford Linear Accelerator Center. An integrated luminosity of 211 fb^{-1}, corresponding to $(231.8\pm2.6)\times10^6$ $B\overline{B}$ pairs, was recorded at the $\Upsilon(4S)$ resonance (center-of-mass energy $\sqrt{s} = 10.58$ GeV).

Charged particles from the e^+e^- interactions are detected, and their momenta measured, by a combination of five layers of double-sided silicon microstrip detectors (SVT) and a 40-layer drift chamber (DCH), both operating in the 1.5-T magnetic field of a superconducting solenoid. Photons and electrons are identified with a CsI(Tl) electromagnetic calorimeter (EMC). Further charged particle identification (PID) is provided by the average energy loss ($\mathrm{d}E/\mathrm{d}x$) in the tracking devices and by an internally reflecting ring imaging Cherenkov detector (DIRC) covering the central region.

Monte Carlo simulation is used to evaluate background contamination and selection efficiency. Signal and background Monte Carlo samples are generated with EvtGen [10]. The detector response is simulated with GEANT4 [11] and all simulated events are reconstructed in the same manner as data.

We reconstruct B meson candidates through the decays $\phi\pi^+$ or $\phi\pi^0$, with $\phi \to K^+K^-$ and $\pi^0 \to \gamma\gamma$. All kaon candidate tracks in the reconstructed decay chains must satisfy a set of loose kaon identification criteria based on the response of the DIRC and the $\mathrm{d}E/\mathrm{d}x$ measurements in the DCH and SVT. In both decay modes, all the tracks coming from the fully reconstructed B are required to originate from the interaction point. A pair of oppositely-charged kaon candidates is considered as a ϕ candidate if its invariant mass is within 15 MeV/c^2 of the nominal ϕ mass value (1019.5 MeV/c^2 [12]). This is about three times the observed width in the K^+K^- invariant mass spectrum. A pair of energy deposits in the EMC, each of which is isolated from any charged track and has the lateral shower shape expected for photons, is considered as a π^0 candidate if both the deposits exceed 40 MeV in the laboratory frame and the associated invariant mass of the pair is between 110 MeV/c^2 and 160 MeV/c^2 (about three times the observed width in the $\gamma\gamma$ invariant mass spectrum). B meson candidates are made by combining ϕ candidates with a charged track or a π^0 candidate. We do not apply any particle identification criteria on the track which comes directly from B meson decay (primary track) at this stage, so for the charged mode we reconstruct $B^+ \to \phi h^+$ ($h^+ = \pi, K$) events. This allows us to study the $B^+ \to \phi K^+$ signal, which is the largest background coming from B decays.

Two kinematic variables are used to discriminate between signal B decays and combinatorial background: the invariant mass of the reconstructed B meson candidate, m_B and $m_{\rm miss} = \sqrt{(q_{e^+e^-} - \tilde{q}_B)^2}$, where $q_{e^+e^-}$ is the four momentum of the initial e^+e^- system and $\tilde{q}_B$ is the mass-constrained four momentum of the re-

constructed B meson candidate. By construction, the linear correlation between $m_{\rm miss}$ and m_B vanishes. Compared to the kinematic variables $\Delta E = E_B^* - \frac{1}{2}\sqrt{s}$ and $m_{\rm ES} = \sqrt{\frac{1}{4}s - p_B^{*2}}$ (where $s = q^2_{e^+e^-}$ and the asterisk denotes the e^+e^- rest frame), which were used in the previous *BABAR* analysis of these modes [6], the present combination of variables has less correlation and better background suppression. The distribution of m_B peaks at the nominal B mass value [12], with a width of about $20\,{\rm MeV}/c^2$ for $\phi\pi^+$, and about $40\,{\rm MeV}/c^2$ for $\phi\pi^0$, with a low-side tail due to energy leakage from the EMC. The resolution on $m_{\rm miss}$ is about $5\,{\rm MeV}/c^2$, dominated by the beam-energy spread. We require m_B to be within 150 ${\rm MeV}/c^2$ of the nominal B mass and $5.11\ {\rm GeV}/c^2 < m_{\rm miss} < 5.31\ {\rm GeV}/c^2$. The region $m_{\rm miss} < 5.2\ {\rm GeV}/c^2$ is used for background characterization.

The dominant background comes from combinatorial $e^+e^- \to q\bar{q}$ ($q = u, d, s, c$) continuum events. They tend to be jet-like in the center-of-mass (CM) frame, while B decays tend to be spherical. To exploit this characteristic for discriminating against continuum background, we use the ratio L_2/L_0, where L_i is defined as

$$L_i = \sum_k |p_k||\cos(\theta_k)|^i, \qquad (1)$$

where p_k is the momentum of particle k, and θ_k is the angle between p_k and the thrust axis of the reconstructed B meson evaluated in the CM frame. The sum runs over the charged and neutral particles of the event not assigned to the B meson. We require $L_2/L_0 < 0.55$, which suppresses the continuum background by more than a factor of 3, while retaining about 90% of the signal. We require $|\cos\theta_B^*| < 0.9$, where θ_B^* is the angle between the B candidate momentum and the e^+ momentum in the CM frame. For B candidates the probability density function of θ_B^* is proportional to $\sin^2\theta_B^*$, whereas for continuum events it is nearly uniform after acceptance. We select events for which one B is reconstructed as $B^+ \to \phi h^+$ or $B^0 \to \phi\pi^0$ and the other B is only partially reconstructed [13]. We define Δt to be the difference between the proper decay times of the B mesons and $\sigma_{\Delta t}$ the uncertainty associated with it. We require, in the case of $B^0 \to \phi\pi^0$ only, $|\Delta t| < 20$ ps and $\sigma_{\Delta t} < 2.5$ ps. These requirements on Δt and $\sigma_{\Delta t}$ retain about 92% of the signal, while removing about 15% of the continuum events. After the application of these selection criteria on Monte Carlo simulated events, the efficiencies for $\phi\pi^+$ and $\phi\pi^0$ signal are $(37.1 \pm 0.1)\%$ and $(29.5 \pm 0.8)\%$ respectively. The average candidate multiplicity in events with at least one candidate is ~ 1.005 for both decay modes. If more than one B candidate is reconstructed in an event, we choose the one with the $\phi \to K^+K^-$ invariant mass closest to the nominal ϕ mass value [12], for $B^+ \to \phi\pi^+$ decays. For $B^0 \to \phi\pi^0$ decays, we choose the candidate with the $\pi^0 \to \gamma\gamma$ invariant mass closest to the nominal π^0 mass value [12]. These criteria produce no bias in the shape of the other event variables used in the maximum likelihood fit described below. We select 10990 and 2732 events in the ϕh^+ and $\phi\pi^0$ analyses respectively.

A possible background to the $\phi \to K^+K^-$ decays comes from the S-wave production of the K^+K^- system ($B \to (K^+K^-)_{\rm S-wave}\pi$ decays) with contributions coming predominantly from resonances such as $f_0(980)$ and $a_0(980)$. Using samples of simulated decays of B mesons equivalent to nearly five times the size of the data sample, we found that all the other B decay modes give negligible sources of background. To discriminate against S-wave background in the maximum likelihood fit, we use the helicity of the K^+K^- system, in terms of the cosine of the angle θ_H between the K^+ candidate and the parent B meson flight direction in the K^+K^- rest frame. The helicity probability density function is proportional to $\cos^2\theta_H$ for the signal, and is uniformly distributed for the S-wave background. Further discrimination is provided by the K^+K^- invariant mass distribution, m_{KK}, which peaks at the ϕ mass for the signal, while it peaks at lower values for the S-wave background.

In the case of charged B decays, we exploit the Cherenkov angle θ_c measured in the DIRC for the primary track, in order to determine simultaneously the yields of $B^+ \to \phi\pi^+$ and $B^+ \to \phi K^+$ decays and the yields of the two corresponding $B^+ \to (K^+K^-)_{\rm S-wave}h^+$ ($h = \pi, K$) background components.

Signal and background yields N_i, where i denotes signal, continuum, and S-wave background, are extracted using an extended maximum likelihood fit with the likelihood function 2:

$$\mathcal{L} = \frac{1}{N!}\exp\left(-\sum_i N_i\right)\prod_{j=1}^{N}\left[\sum_i N_i \mathcal{P}_i(\vec{x_j};\vec{\alpha}_i)\right]. \qquad (2)$$

where N is the total number of events entering the fit. The probabilities $\mathcal{P}_i$ are products of Probability Density Functions (PDF) for each of the independent variables $\vec{x} = \{m_{\rm miss}, m_B, L_2/L_0, m_{KK}, \cos\theta_H\}$. In the case of $B^+ \to \phi h^+$ the variable θ_c is also used in the fit. The $\vec{\alpha}_i$ are the parameters of the PDFs for $\vec{x}$. By minimizing the quantity $-\ln\mathcal{L}$ in two separate fits, we determine the yields for $\phi\pi^+$ and $\phi\pi^0$. There are three B backgrounds to $B^+ \to \phi\pi^+$ decay ($B^+ \to (K^+K^-)_{\rm S-wave}h^+$ and $B^+ \to \phi K^+$), while only $B^0 \to (K^+K^-)_{\rm S-wave}\pi^0$ contributes to the $B^0 \to \phi\pi^0$ mode. All the yields in Eq. 2 are allowed to fluctuate to negative values in the fits.

The distributions of L_2/L_0 and $\cos\theta_H$ are described by a parametric step function [14] and a second-order polynomial respectively. We use a Gaussian for the $m_{\rm miss}$ distribution for $\phi\pi^+$ signal and S-wave components, a Gaussian with exponential tails for the m_B distribution

for $\phi\pi^+$ signal and S-wave components, and for both $m_{\rm miss}$ and m_B for $\phi\pi^0$ signal and S-wave components. For the continuum $m_{\rm miss}$ distribution we use the function $x\sqrt{1-x^2}\exp\left[-\xi(1-x^2)\right]$, with $x \equiv 2m_{\rm miss}/\sqrt{s}$ and ξ a floating parameter. The m_{KK} invariant mass distribution is described by a relativistic Breit-Wigner function for signal, a relativistic Breit-Wigner plus exponential for the continuum background and a Flatté [15, 16] function for the S-wave background. The Flatté function takes into account the coupling of the scalar resonances to the $\pi^+\pi^-$ and K^+K^- channels [17].

The θ_c PDFs are obtained from a large data sample of $D^{*+} \to D^0\pi^+$ ($D^0 \to K^-\pi^+$) decays where $K^\mp/\pi^\pm$ tracks are identified through the charge correlation with the $\pi^\pm$ from the $D^{*\pm}$ decay. The PDFs are constructed separately for K^+, K^-, π^+ and π^- tracks as a function of momentum and polar angle using the expected values of θ_c, and its uncertainty.

The continuum parameters are allowed to vary, except for the $m_{\rm miss}$ end-point. All other parameters are fixed to their values derived from data control samples. These are varied within their uncertainties to evaluate the systematic error.

Using a large number of simulated experiments, we find that the usual maximum likelihood fitting technique does not provide an unbiased estimate of the true values of signal and S-wave yields (N_S and $N_{\rm S-wave}$) because of the non-Gaussian shape of the likelihood function when the yield is very small. Therefore we use a Bayesian statistical approach to obtain a modified likelihood function $L(N_S)$:

$$L(N_S) = N_0 \int_0^\infty dN_{\rm S-wave}\mathcal{L}(N_S, N_{\rm S-wave}), \qquad (3)$$

where the normalization N_0 is such that $\int_0^\infty dN_S L(N_S) = 1$. The two dimensional likelihood $\mathcal{L}(N_S, N_{\rm S-wave})$ is given at each point on the $N_S - N_{\rm S-wave}$ plane by the function defined in Eq. 2, maximized with respect to all of the other fit variables. When seeking the central value for the branching fraction we take the median of L, with the lower limit replaced by $-\infty$ and N_S unrestricted. This is because we find from simulations that in the case of very low yields, the median provides a less biased estimator of the true value of N_S than the maximum of L. We correct the central value of the branching fractions for the residual biases. When calculating upper limits, we impose the *a priori* constraints $N_S > 0$ and $N_S - wave > 0$.

Fig. 2 shows the $m_{\rm miss}$ and m_B distributions for data, with the PDF corresponding to the maximum likelihood fit overlaid. We do not observe evidence for either $B^+ \to \phi\pi^+$ or $B^0 \to \phi\pi^0$ decays.

The signal yields, extracted from the median of the likelihood $L(N_S)$ (Eq. 3), are reported in Table I. In the case of $B^+ \to \phi\pi^+$, we also measure the $N_{\phi K^+}$ yield, which is found to be compatible with the expectation from published branching fractions [5].

TABLE I: Signal yield (evaluated as the median of the likelihood), detection efficiency ε (the uncertainty includes both statistical and systematic effects), measured branching fraction $\mathcal{B}$ with statistical error, after the correction for the fit bias has been applied, for the two decay modes considered and upper limit at 90% probability.

	$B^+ \to \phi\pi^+$	$B^0 \to \phi\pi^0$
Yield	-1.5 ± 5.9	4.0 ± 3.5
$\varepsilon(\%)$	37.1 ± 0.1	29.5 ± 0.8
$\mathcal{B}(10^{-6})$	-0.04 ± 0.17	0.12 ± 0.13
UL$(\mathcal{B})(10^{-7})$	2.4	2.8

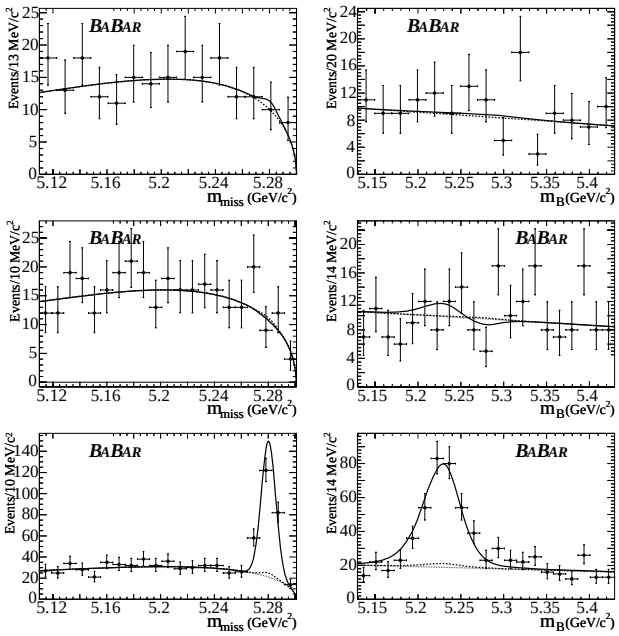

FIG. 2: Distribution of $m_{\rm miss}$ (left) and m_B (right) for reconstructed $B^0 \to \phi\pi^0$ (top plots), $B^+ \to \phi\pi^+$ (middle plots) and $B^+ \to \phi h^+$ ($h = \{\pi, K\}$) (bottom plots), after applying a requirement on the ratio of signal likelihood to signal-plus-background likelihood to enhance the signal. The curves are projections from the likelihood fit for total yield (solid line), for the continuum background (fine dashed line) and for continuum plus S-wave component (dashed line). For $B^+ \to \phi h^+$ decay we don't apply any particle identification criteria and assign the pion mass to the primary track. For this reason, the m_B distribution for $B^+ \to \phi K^+$ events is shifted with respect to the nominal B^+ mass (positive bump in middle and bottom plot), while it peaks at the nominal value for $B^+ \to \phi\pi^+$ events (negative bump in middle plot).

The branching fraction $\mathcal{B}$ is calculated from the observed number of signal events as

$$\mathcal{B} = \frac{N_S}{\varepsilon \cdot N_{B\bar{B}} \cdot \mathcal{B}(\phi \to K^+K^-)} \qquad (4)$$

where $N_{B\bar{B}}$ is the number of $B\bar{B}$ pairs produced and

TABLE II: Summary of systematic uncertainties contributing to the total error for the upper limit on the branching fraction. They are given in units of 10^{-8}.

	$B^+ \to \phi\pi^+$	$B^0 \to \phi\pi^0$
PDF Uncertainty	$^{+1.9}_{-2.8}$	$^{+3.6}_{-4.2}$
PID Efficiency	0.1	0.1
Tracking Efficiency	0.1	0.2
π^0 Efficiency	-	0.1
L_2/L_0 Cut	0.1	0.3
$B\bar{B}$ Pair Counting	0.1	0.2
Interference Effects	0.3	0.6
$\mathcal{B}(\phi \to K^+K^-)$, $\mathcal{B}(\pi^0 \to \gamma\gamma)$	0.1	0.1
Total	$^{+2.8}_{-3.6}$	$^{+3.7}_{-4.3}$

ε is the reconstruction efficiency for the B candidates. In Eq. 4 we assume equal branching fractions for $\Upsilon(4S)$ decays to charged and neutral B-meson pairs [18].

The systematic uncertainties are summarized in Table II. The uncertainty arising from the lack of knowledge of continuum background PDFs is part of the statistical error since the background parameters are free to vary in the fit. The uncertainty on the signal PDFs represents the dominant error. We estimate it by using simulated and high-statistics data control samples of $B^+ \to \pi^+\overline{D}^0$ ($\overline{D}^0 \to K^+\pi^-$) and $B^0 \to \pi^+D^-$ ($D^- \to K^0_S\pi^-$) events. In order to estimate the systematic uncertainty on m_B for $B^0 \to \phi\pi^0$ we use a data control sample of $B^+ \to h^+\pi^0$ events. The control channels have event topologies similar to those of $B^+ \to \phi h^+$ and $B^0 \to \phi\pi^0$. We use them to determine the signal PDF parameters and take the difference in yields found by varying these parameters within one standard deviation as the systematic error. The second most important error comes from the uncertainty on the efficiency ε. The track detection efficiency uncertainty is estimated to be 0.8% per track from a study of a variety of control samples, such as $\tau \to$ 3-track decays. We assign 0.5% uncertainty on the kaon identification efficiency. The uncertainty on the reconstruction efficiency for the π^0 is 3%, as measured in a large sample of $\tau^- \to \rho^-\nu_\tau$, $\rho^- \to \pi^-\pi^0$ decays coming from $e^+e^- \to \tau^+\tau^-$. We assign a 1.8% uncertainty on the L_2/L_0 cut efficiency, estimated by the difference between Monte Carlo and data control samples, 1.1% on the total number of $\Upsilon(4S) \to B\bar{B}$ decays in the sample and 1.2% on the knowledge of $\mathcal{B}(\pi^0 \to \gamma\gamma)$ and $\mathcal{B}(\phi \to K^+K^-)$. We estimate the systematic error introduced by the approximation of ignoring interference effects between the ϕ and the K^+K^- S-wave components by varying the relative strong phases and taking the largest observed variation as the error. In this study we include the $f_0(980)$ resonance and a non-resonant component, whose contribution is taken from a $B^+ \to K^+K^-K^+$ Dalitz plot measurement by the Belle Collaboration[19]. The resulting uncertainty is 4.4% for both modes.

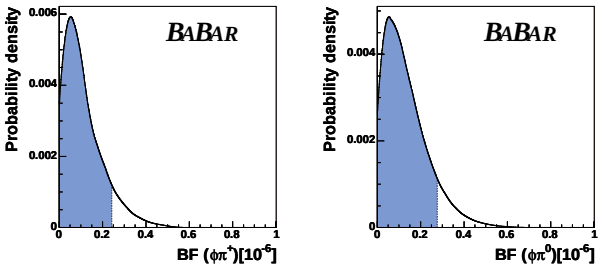

FIG. 3: Likelihood distribution, $L_\mathcal{B}(\mathcal{B})$, for $\mathcal{B}(B^+ \to \phi\pi^+)$ (left) and $\mathcal{B}(B^0 \to \phi\pi^0)$ (right). The upper boundary of the dark region represents the 90% probability upper limit.

Under the assumption that $N_{B\bar{B}}$ and ε are distributed as Gaussians, we obtain a likelihood function, $L_\mathcal{B}$, for the branching fraction, $\mathcal{B}$, based on Eq. 4, by convolving the likelihood (L in Eq. 3) with the distributions of $N_{B\bar{B}}$ and ε. We also include the additional uncertainty coming from the systematic error on the signal yield. The resulting likelihood is shown in Fig. 3 for each of the two decay modes. In the plots, the upper boundary of the dark region represents the 90% probability Bayesian upper limit $\mathcal{B}_{\rm UL}$, defined as:

$$\int_0^{\mathcal{B}_{\rm UL}} L_\mathcal{B}(\mathcal{B})d\mathcal{B} \;=\; \frac{9}{10}\int_0^{+\infty} L_\mathcal{B}(\mathcal{B})d\mathcal{B} \qquad (5)$$

We determine $\mathcal{B}(B^+ \to \phi\pi^+) < 2.4 \times 10^{-7}$ and $\mathcal{B}(B^0 \to \phi\pi^0) < 2.8 \times 10^{-7}$.

We compute the central values for the branching fractions by correcting the fitted signal yields for the fit bias, estimated using a large number of simulated experiments, and including a systematic uncertainty equivalent to half the fit bias. This error corresponds to a shift of -0.8 and -0.4 events in the signal yield, and -1.9×10^{-8} and -1.2×10^{-8} in the branching fraction for $B^+ \to \phi\pi^+$ and $B^0 \to \phi\pi^0$, respectively. Without taking into account the *a priori* knowledge of $N_S > 0$ and $N_{\rm S-wave} > 0$, and integrating the likelihood in Eq. 3 around the median, we obtain as 68%-probability regions $\mathcal{B}(B^+ \to \phi\pi^+) = (-0.04 \pm 0.17) \times 10^{-6}$ and $\mathcal{B}(B^0 \to \phi\pi^0) = (0.12 \pm 0.13) \times 10^{-6}$. The results are summarized in Table I.

In summary we have searched for $B^+ \to \phi\pi^+$ and $B^0 \to \phi\pi^0$ decays in a sample of 232 million $B\overline{B}$ meson pairs. We find no evidence of signal and therefore we place upper limits $\mathcal{B}(B^+ \to \phi\pi^+) < 2.4 \times 10^{-7}$ and $\mathcal{B}(B^0 \to \phi\pi^0) < 2.8 \times 10^{-7}$ at 90% probability. These limits are more stringent than earlier results [5–7] and they supersede our previous publications [5, 6]. They are consistent with existing SM predictions [1].

We are grateful for the excellent luminosity and machine conditions provided by our PEP-II colleagues, and for the substantial dedicated effort from the computing

organizations that support *BABAR*. The collaborating institutions wish to thank SLAC for its support and kind hospitality. This work is supported by DOE and NSF (USA), NSERC (Canada), IHEP (China), CEA and CNRS-IN2P3 (France), BMBF and DFG (Germany), INFN (Italy), FOM (The Netherlands), NFR (Norway), MIST (Russia), and PPARC (United Kingdom). Individuals have received support from CONACyT (Mexico), Marie Curie EIF (European Union), the A. P. Sloan Foundation, the Research Corporation, and the Alexander von Humboldt Foundation.

* Also at Laboratoire de Physique Corpusculaire, Clermont-Ferrand, France
† Also with Università di Perugia, Dipartimento di Fisica, Perugia, Italy
‡ Also with Università della Basilicata, Potenza, Italy

[1] S. Bar-Shalom, G. Eilam and Y. D. Yang, Phys. Rev. D **67**, 014007 (2003).
[2] Throughout this paper, charge conjugate reactions are included implicitly and ϕ refers to the $\phi(1020)$.
[3] See for example A. J. Buras and L. Silvestrini, Nucl. Phys. B **569** 3 (2000).
[4] Y. Grossman *et al.*, Phys. Rev. D **68**, 015004 (2003).
[5] *BABAR* Collaboration, B. Aubert *et al.*, Phys. Rev. D **69** 011102 (2004).
[6] *BABAR* Collaboration, B. Aubert *et al.*, Phys. Rev. D **70** 032006 (2004).
[7] CLEO Collaboration, T. Bergfeld *et al.*, Phys. Rev. Lett. **81**, 272 (1998).
[8] *BABAR* Collaboration, B. Aubert *et al.*, Nucl. Instr. Methods Phys. Res., Sect. A **479**, 1 (2002).
[9] PEP-II Conceptual Design Report, SLAC-R-418 (1993).
[10] D. J. Lange, Nucl. Instr. Methods Phys. Res., Sect. A **462**, 152 (2001).
[11] GEANT Collaboration, S. Agostinelli *et al.*, Nucl. Instr. Methods Phys. Res., Sect. A **506**, 250 (2003).
[12] Particle Data Group, S. Eidelman *et al.* Phys. Lett. B **592**, 1 (2004).
[13] *BABAR* Collaboration, B. Aubert *et al.* Phys. Rev. D **71**, 091102 (2005)
[14] *BABAR* Collaboration, B. Aubert *et al.*, Phys. Rev. Lett. **91**, 241801 (2003).
[15] S. Flatté, Phys. Lett. B **63**, 224 (1976).
[16] V. Baru, J. Haidenbauer, C. Hanhart, A. Kudryavtsev and U. G. Meissner, Eur. Phys. J. A **23**, 523 (2005).
[17] X. Shen, Int. J. Mod. Phys. A **20** 1706 (2005).
[18] *BABAR* Collaboration, B. Aubert *et al.*, Phys. Rev. D **69**, 071101 (2004).
[19] Belle Collaboration, A. Garmash *et al.*, Phys. Rev. D **71**, 092003 (2005).